Temporal Coherence Envelope Function for Field Emission in Electron Microscopy

Xuan Tan Nguyen and Michael S. Altman

Department of Physics, Hong Kong University of Science and Technology, Hong Kong SAR, China

Funded by the Hong Kong Research Grant Council (#16304718)

Abstract: Partial electron spatial and temporal coherence arise from the divergence and energy spread of the electron beam, respectively. The theoretical treatment of temporal coherence pioneered by Hanßen and Trepte fifty years ago [1] assumes a Gaussian energy distribution. However, state-of-the art instruments employ field emission (FE) sources that emit electrons with a non-Gaussian energy distribution. We have updated earlier work to describe the temporal coherence of a FE energy distribution. The updated description is implemented in Fourier optics simulations to explore the effect of FE on image formation in non-aberration-corrected (NAC) and aberration-corrected (AC) low energy electron microscopy (LEEM). Although the resolution that can be achieved for the FE distribution is only slightly degraded compared to a Gaussian distribution with the same energy spread, FE does produce a noticeable focus offset. These insights are valuable for carrying out quantitative evaluations of contrast in focal image series to determine details of sample structure and to characterize source divergence. The approach developed here is similarly applicable to transmission electron microscopy.

Fourier Optics [2-5]

- The wave emitted by the sample is described by an objection function, $\psi_o(\mathbf{r}) = \sigma(\mathbf{r})\exp(i\phi(\mathbf{r}))$, where $\sigma(\mathbf{r})$ and $\phi(\mathbf{r})$ are the amplitude and phase.
- Imaging errors caused by the instrument are included by modifying the Fourier transform of the object function, $\Psi(q)$, where $q = \alpha/\lambda$ is the spatial frequency, α is the emission angle from the object, and λ is the electron wavelength .
- The image intensity is given by

$$I(\mathbf{r}) = \iint \Psi(\mathbf{q})\Psi^*(\mathbf{q}')R(\mathbf{q},\mathbf{q}',\Delta z)\exp(i2\pi(\mathbf{q}-\mathbf{q}')\cdot\mathbf{r})d\mathbf{q}d\mathbf{q}'$$

where Δz is defocus and the composite contrast transfer function describes how information at different spatial frequencies is transmitted by the instrument

$$R(\mathbf{q},\mathbf{q}',\Delta z) = M(q)\,M^*(q')\,W_S(q,\Delta z)\,W_S^*(q',\Delta z)\,E_C(q,q')\,E_S(\mathbf{q},\mathbf{q}',\Delta z)$$

The aperture function: $M(q) = \begin{cases} 1 & \text{for } |q| < q_{ap} \\ 0 & \text{for } |q| \geq q_{ap} \end{cases}$

The wave aberration function:

$$W_S(q,\Delta z) = exp\left(i2\pi\chi_S(q,\Delta z)\right)$$

$$\chi_S(q,\Delta z) = \frac{1}{4}C_3\lambda^3q^4 + \frac{1}{6}C_5\lambda^5q^6 - \frac{1}{2}\Delta z\lambda q^2$$

C_3, C_5 are 3rd and 5th order spherical aberration coefficients

The envelope functions: E_C and E_S describe damping caused by partial temporal and partial spatial coherence, respectively.

Temporal Coherence Envelope Function

- The temporal coherence envelope function for an arbitrary energy distribution is the weighted sum of envelope functions for the individual Gaussian distributions that comprise a multi-Gaussian sum approximation

$$E_{C(N)}(q,q') = \sum_{n=1}^{N} A_n E_{C,n}(q,q')$$

where

$$E_{C,n}(q,q') = E_{CC,n}(q,q')\exp\left(-2\pi^2\sigma_{E,n}^2E_{CC,n}^2(q,q')d_n^2 - \frac{\varepsilon_n^2}{2\sigma_{E,n}^2}\right)$$

$$E_{CC,n}(q,q') = \left[1 - i4\pi b_2\sigma_{E,n}^2\right]^{-1}$$

$$d_n = b_1 - i\frac{\varepsilon_n}{2\pi\sigma_{E,n}^2} \qquad b_2 = \frac{C_{CC}\lambda(q^2-q'^2)}{2E^2}$$

$$b_1 = \frac{C_C\lambda(q^2-q'^2)}{2E} + \frac{C_{3C}\lambda^3(q^4-q'^4)}{4E}$$

C_C, C_{CC}, and C_{3C} are 2nd, 3rd, and 4th rank chromatic aberration coefficients

- The real (red) and imaginary (blue) components of the envelope functions for the FE distribution (solid lines) and Gaussian distribution (dashed lines) with the same energy spread are shown below for NAC and AC LEEM. Aberration coefficients for the IBM LEEM at imaging energy E_0 = 10 eV [3] are used.

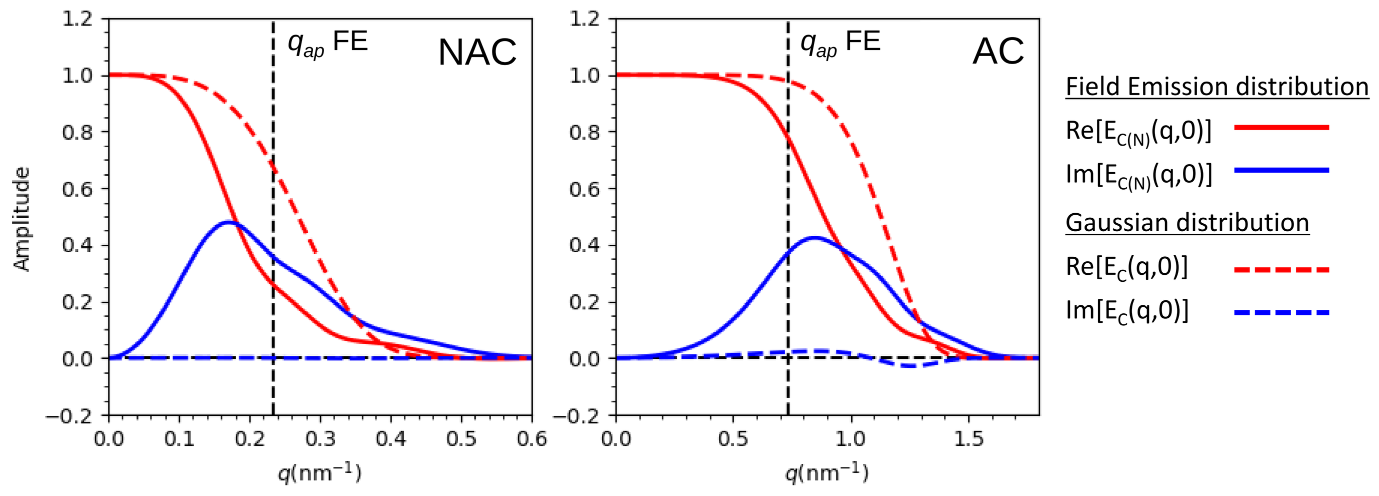

Field Emission Energy Distribution

- An arbitrary energy distribution is approximated by a weighted sum of N Gaussian functions

$$c(\varepsilon) = \sum_{n=1}^{N} A_n c_n(\varepsilon) = \sum_{n=1}^{N} \frac{A_n}{\sqrt{2\pi\sigma_{E,n}^2}} exp\left(-\frac{(\varepsilon-\varepsilon_n)^2}{2\sigma_{E,n}^2}\right)$$

where A_n, $\sigma_{E,n}$, and ε_n are the amplitude, standard deviation, and centroid position of the n^{th} Gaussian in the sum, respectively. The energy spread of a Gaussian distribution is the full-width-half-maximum, $\Delta E = 2\sigma_E\sqrt{2\ln 2}$.

- The field emission (FE) distribution from tungsten at 300K with energy spread ΔE = 0.242 eV given by the Fowler-Nordheim model [6] is approximated by a triple Gaussian sum.

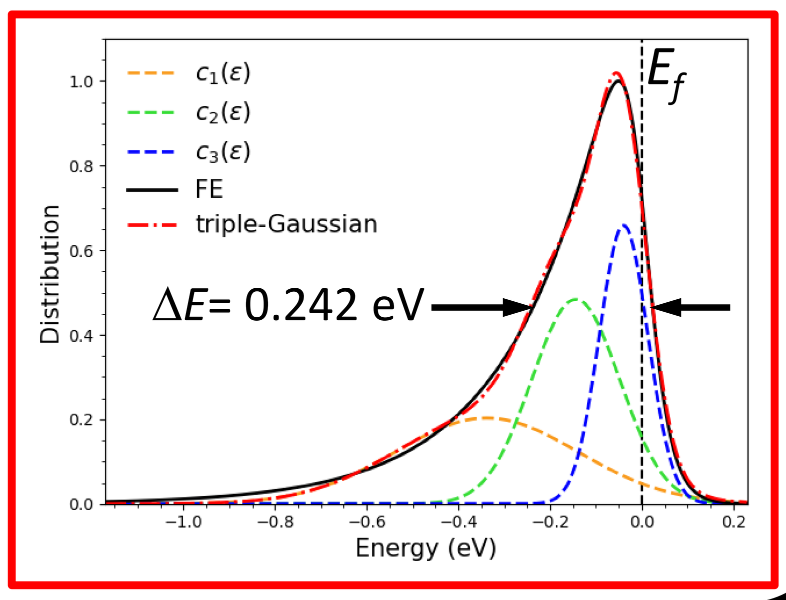

Results: Focus Offset, Resolution

- Fourier optics simulations of a $\phi = 3\pi/2$ step phase object and $1{:}\sqrt{2}/2$ amplitude object were performed for Gaussian and Field emission energy distributions. The IBM LEEM instrument parameters at imaging energy E_0 = 10 eV [3] were used. The step phase object represents an atomic surface step. The amplitude object represents the boundary between regions with different structure.
- The $\phi = 3\pi/2$ step phase object produces asymmetric interference fringes that reverse between underfocus (Δz<0) and overfocus (Δz>0) conditions. This phenomena identifies a focus offset between imaging with FE and Gaussian energy distributions.

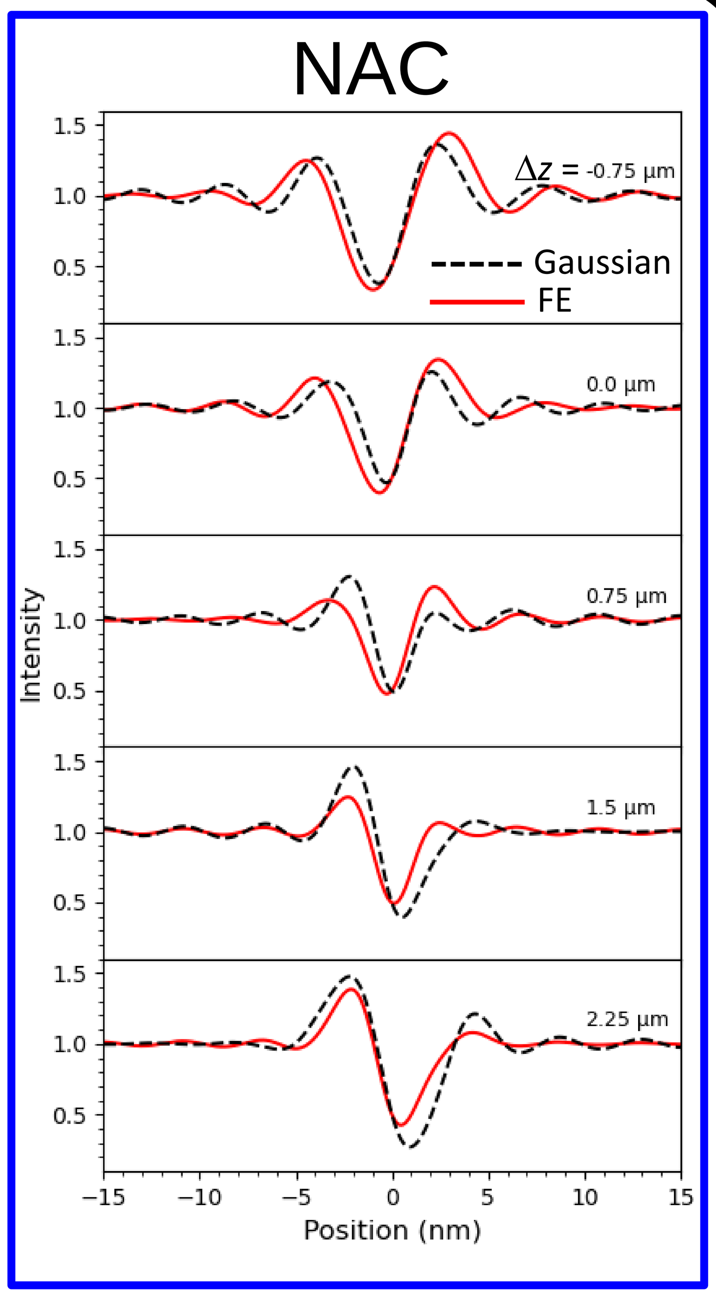

- The resolution is determined by the 84/16 condition for the amplitude object [3]. The resolution at the in-focus condition, Δz = 0, is degraded for the FE distribution. The resolution improves at positive defocus because defocus compensates spherical aberrations at the Scherzer defocus, ΔZ_S [3,7]. The dependence of resolution on defocus also demonstrates the focus offset. These effects are weaker for AC than NAC.

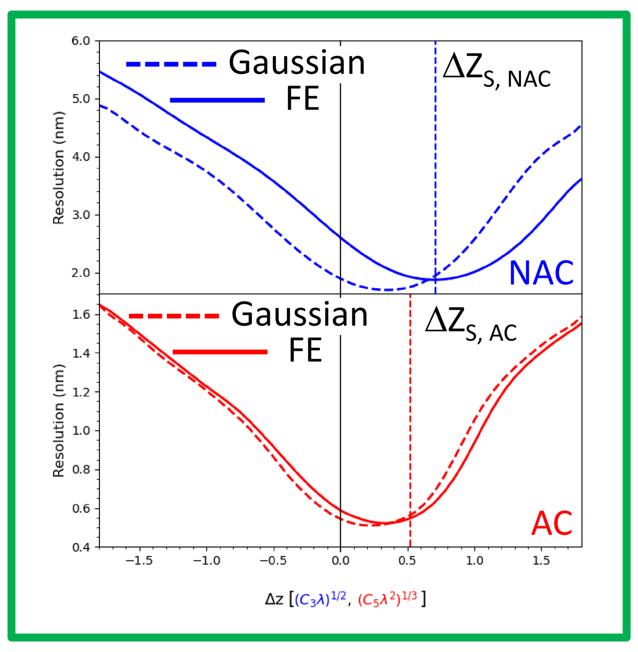

References

[1] K.J. Hanßen, L. Treptke, Optik **32** (1971) 519.
[2] A.B. Pang, T. Müller, M.S. Altman, E. Bauer, J. Phys.: Condens. Matter **21** (2009) 314006.
[3] S.M. Schramm, A.B. Pang, M.S. Altman, R.M. Tromp, Ultramicroscopy, **115** (2012) 88.
[4] J.C.H. Spence, *High Resolution Electron Microscopy*, 4th ed. (Oxford University Press, Oxford, 2013)
[5] K.M. Yu, K.L.W. Lau, M.S. Altman, Ultramicroscopy **200** (2019) 160.
[6] R. D. Young, Phys. Rev. **113** (1959) 110.
[7] O. Scherzer, J. Appl. Phys. **20** (1949) 20.